© 2015. Published by The Company of Biologists Ltd | The Journal of Experimental Biology (2015) 218, 664-667 doi:10.1242/jeb.111013

SHORT COMMUNICATION

Erection pattern and section-wise wettability of honeybee glossal hairs in nectar feeding

Jianing Wu[1,*], Rengao Zhu[1,2,*], Shaoze Yan[1,‡] and Yunqiang Yang[2]

ABSTRACT

The honeybee's tongue (glossa) is covered with bushy hairs and resembles a mop or a brush. We examined the dimensions of glossal hairs of the Italian honeybee (*Apis mellifera ligustica*) and found that the average length of hairs increased from the proximal segment to the distal end. The glossal dynamic surface of a honeybee in drinking cycles was captured by a specially designed high-speed camera system, and we discovered that the glossal hairs erected rhythmically when drinking nectar; specifically, hairs on the proximal segment erected earlier than those on the distal end of a honeybee's tongue, which was identified as the phenomenon of asynchronous hair erection. Moreover, by measuring the wettability of the tongue, we found that the flabellum was the most hydrophilic and the root of the tongue was hardest to be wetted. According to our observations, we suggest that the honeybee has an optimal hair-erection pattern that could balance nectar intake and viscous drag. These results will be helpful to understand the liquid-feeding mechanism of honeybees, especially the role of erectable glossal hairs.

KEY WORDS: Honeybee, Asynchronous hair erection, Section-wise wettability, Nectar feeding

INTRODUCTION

The drinking patterns of animals such as cats (Reis et al., 2010), dogs (Crompton and Musinsky, 2011), bats (Harper et al., 2013) and hummingbirds (Kim et al., 2012; Rico-Guevara and Rubega, 2010) have been observed and analysed explicitly to varying degrees in previous studies. The dynamic surfaces, categorized as the erectable hairs, setae and filamentous papillae, play an important role in improving the ability of trapping liquid food (Harper et al., 2013). A honeybee is a typical insect whose proboscis has been studied widely, for instance, in relation to gustation preferences (Heyneman, 1983; Tan et al., 2014) and nectar lapping strategies (Yang et al., 2014). The mouthpart of a honeybee that functions in nectar feeding comprises a pair of galeae, a pair of labial palpi and a bushly hairy glossa (Krenn et al., 2005).While drinking nectar, its galeae and labial palpi form a sucking tube, and the tongue (glossa) inside produces a dipping motion based on forward protraction and backward retraction to load nectar as it is sucked. The glossa resembles a mop covered by bushy hairs, which helps it transport nectar more efficiently (Yang et al., 2014). Recently, Harper et al. (2013) discovered that a nectar-feeding bat, *Glossophaga soricina*, uses dynamic erectile papillae driven hemodynamically to collect nectar. Inspired by this, we speculate that the glossa of the honeybee might erect hairs in a specific pattern for nectar dipping. However, characteristics of the erection pattern of glossal hairs have been a highly controversial issue until now, which is not clearly defined because of the relatively small mouthpart sizes and/or high intake rates of the honeybees (Harper et al., 2013; Snodgrass, 1956).

In this study, we sought to identify the feature of glossal hair erection of the honeybee in nectar feeding and explore the benefit of this preferred erection pattern. We first observed the hair-equipped microstructure on the surface of the glossa, then recorded and analysed the erection behaviour of glossal hairs in the drinking process of honeybees experimentally using a high-speed camera system (Fig. 1A). We suggest that the specific pattern of glossal hairs in nectar feeding improves the volume of nectar intake and reduces viscous drag.

RESULTS AND DISCUSSION

With the help of a scanning electron microscope (SEM), we observed the microstructure of the mouthpart of the Italian bee *Apis mellifera ligustica*, particularly the surface of the glossa. The glossa was generally shaped as a long and multi-segmental cylinder covered with bushy bristles, and its distal apex was shaped as a spoon-like flabellum (Fig. 1B–G). Notably, the basal surface of the glossa had shorter stiff scales, whereas transverse rings that bore long cuticular hairs dominated the middle and the apical regions. Dimensional parameters of the glossa and hairs can be measured directly by the scale bars in Fig. 1D,F,G. As shown in Fig. 1B,C we subdivided the tongue exposed to the nectar into three uniform sections when it reached the maximum extension as sections I–III, namely the proximal region, middle region and distal region. Each section was 33.3 µm in height, meaning that the lower edge of section III just reached the anterior edge of the glossa. We measured and averaged lengths of the glossal hairs in sections I–III. The lengths of the bristles were 109.47±8.96 µm, 110.57±5.97 µm and 126.61±13.73 µm, respectively. Notably, each segment of the glossa had around 16–20 hairs attached on its surface and was approximately 23 µm along the axial direction. We thus calculated the distribution density of hairs as approximately 2500 mm^{-2}, which indicates just how many hairs grow on such a tiny organ.

Movements and changes of the dynamic glossal surface occurred rapidly in *Apis mellifera ligustica*. We analysed the high-speed photographs frame by frame and found that the whole period of glossa movement for dipping nectar was about 400 ms in our lab environment. We selected six typical drinking events from 50 ms to 100 ms, as shown in Fig. 1H, in which the glossal hairs erected rhythmically. The first panel shows the shape of a glossa when it extends maximally into the nectar and an important feature is that the glossal hairs are not erected until the end of the protraction process. At the time interval between 50 ms and 80 ms, the glossa keeps still but the glossal hairs change their orientation gradually

[1]Division of Intelligent and Biomechanical Systems, State Key Laboratory of Tribology, Department of Mechanical Engineering, Tsinghua University, Beijing 100084, People's Republic of China. [2]School of Engineering and Technology, China University of Geosciences, Beijing 100083, People's Republic of China.
*These authors contributed equally to this work

‡Author for correspondence (yansz@mail.tsinghua.edu.cn)

Received 26 July 2014; Accepted 18 December 2014

The Journal of Experimental Biology

The Journal of Experimental Biology (2015) 218, 664-667 doi:10.1242/jeb.111013

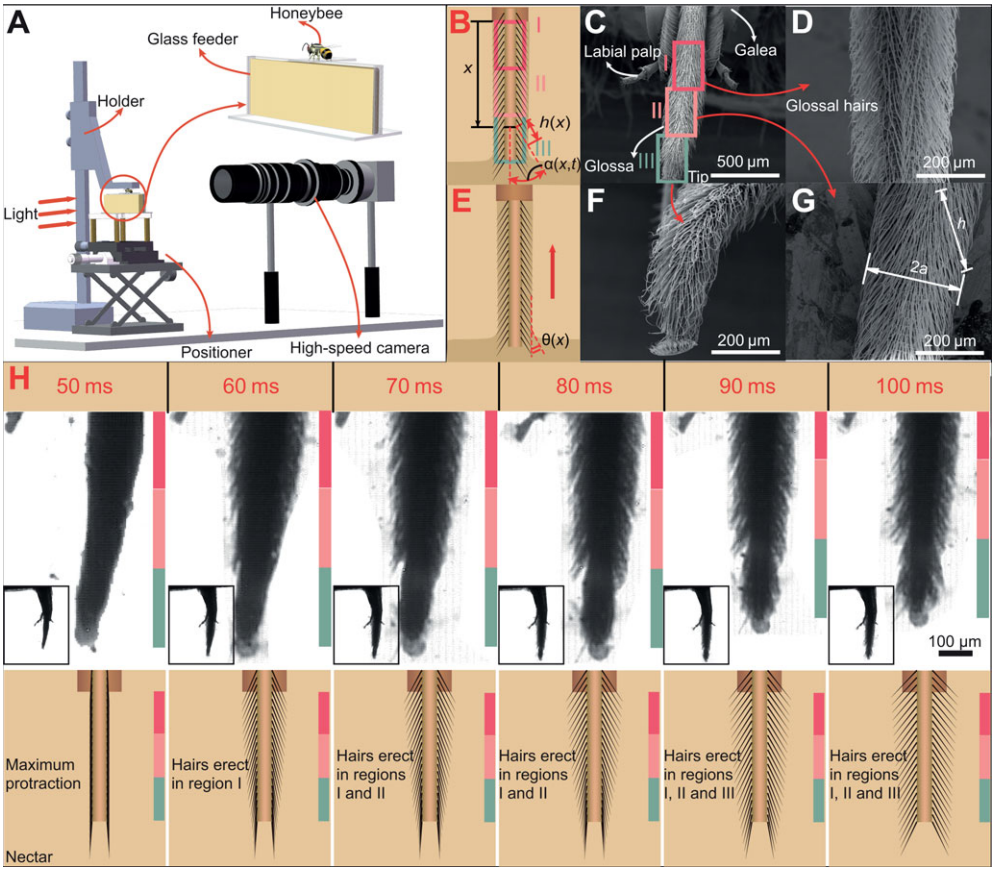

Fig. 1. Experimental setup, microstructure of the glossa surface and movement kinematics of the glossal hairs. (A) Experimental setup. The system comprised a positioner, holder, light source, glass feeder containing sucrose solution and a high-speed camera with a microscope. (B,E) A physical model of the glossa for nectar dipping. When the glossa reaches the maximum protracting position, the exposed part of the glossa is about 1.5 mm long, which can be subdivided uniformly as sections I to III from tip to root of the tongue, with each section 500 μm tall. The contact angle, θ, can be scanned by measuring the meniscus shape. (C,D,F,G) Post mortem examination of the honeybee mouthparts by SEM. (C) Full view of the mouthpart. (D) Basal part of the glossa. (F) Anterior part of the glossa, a spoon-like flabellum sheltered by bristles and sensilla. (G) Zoomed-in view of the middle hairy glossa. (H) Hair erection in feeding *Apis mellifera ligustica* and both the dorsal and ventral surfaces of the tongue are in the camera's field of view. Top panel shows frames from a high-speed movie over 100 ms (supplementary material Movie 1). Bottom panel shows line tracings of the bushy-hair-equipped tongue and nectar. Glossal hairs erect in separate sections step by step and perform asynchronous erection.

from the proximal segment to the distal end. Only hairs in section I erect at 60 ms, whereas hair erection can be observed in both sections I and II at 70 ms. As time goes on, it can be clearly seen in the movie frames that glossal hairs erect in all sections after 90 ms. Then the glossa start withdrawing to load nectar into the sucking tube at 90 ms and the hairs distributed on the tip are totally erect at 100 ms. Further details about the process of nectar uploading can be seen in supplementary material Table S1.

The galeae and labial palpi surrounded the glossa, but only 1 mm of the glossa from the flabellum was immersed in the nectar that was captured by the camera. We measured independent protraction events of five honeybee samples and averaged the erection angles with respect to time. The plot in Fig. 2A indicates that the honeybee exhibits steady kinematics of hair erection. It was observed that hairs on the distal end did not keep pace with those on the proximal segment, and the basal hairs (regions A, D, Fig. 2A) erected first, then the middle hairs (regions B, E, Fig. 2A) and the anterior hairs (regions A, D, Fig. 2A) erected sequentially. We defined this as an asynchronous erection pattern. The ascending order of the total time taken for hair erection was first the basal hairs (regions A, D, Fig. 2A), then the middle hairs (regions B, E, Fig. 2A) and finally the anterior hairs (regions A, D, Fig. 2A). Unlike the nectarivorous bat reported by Harper et al. (2013), the orientation of hairs was not perpendicular to the long axis of the tongue and final erection angles on different regions were not uniformly arranged: the average erection angles of regions A–F were 35.54°, 30.26°, 31.76°, 43.53°, 43.03°, 39.47°, respectively (Harper et al., 2013). Notably, hairs on the dorsal part erected more than those distributed at the ventral part.

We then measured the wettability of the different regions on the glossa with 25%, 35% and 45% (wt/wt) sucrose solution, which suggested that a smaller contact angle indicates higher wettability. The contact angles measured in different glossal regions are shown in Fig. 2B. Viscosity rises sharply when sucrose concentration increases (Yang et al., 2014; Song and Zheng, 2014). So when we used high concentrations of sucrose solution, the viscosity became higher as well. We discovered that, for one part, the contact angles were getting smaller when we used the higher concentration sugar solution, which suggests that the glossa surface exhibits stronger hydrophilicity to the thicker nectar. However, the order of section-wise hydrophilicity remained unchanged as region D>region A, region E>region B and region F>region C under different concentrations of sugar water. The standard deviation shows the boundaries of the error in measuring the section-wise wettability of the glossa. It can be concluded that the dorsal part was much easier to wet than the ventral part. Moreover, the tongue tip was more hydrophilic than the middle region of the tongue and the proximal segment was hardest to wet with the artificial nectar.

The asynchronous erection of glossal hairs might be caused by the variations in the internal pressure of the humor cavity of metameric glossa, which is compressed by the muscular rod (Snodgrass, 1956). In this article, we focused on the function of the asynchronous erection of glossal hairs and tried to explore its role in improving feeding efficiency of honeybees. According to the erection pattern and the section-wise wettability of the glossa, some implications can be drawn. First, the glossal surface, covered by dense hairs, performed wettability of hydrophilicity in that the contact angles were all less than 90°. The volume of nectar collected during lapping is thus directly related to the dimensions of the tongue, as well as the thickness of the adhered-nectar layer (Kim et al., 2011). The nectar intake mass Q can be expressed as: $Q = \rho_{nec} \int_0^X h^2(x) sin^2\alpha(x) dx$, with the assumption that the tongue has the ability to entirely fill gaps between the glossal hairs with nectar, in

The Journal of Experimental Biology

The Journal of Experimental Biology (2015) 218, 664-667 doi:10.1242/jeb.111013

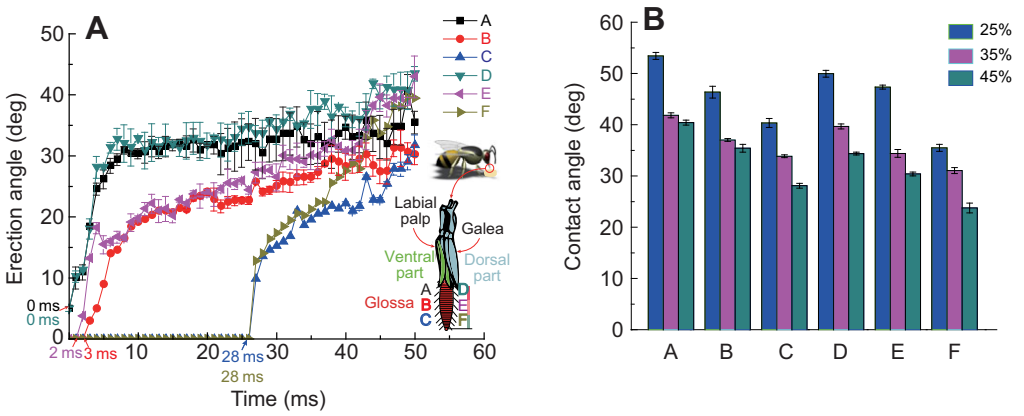

Fig. 2. Asynchronous erection of the glossal hairs and the section-wise wettability of the glossa. (A) Mean±s.d. values of three independent erection angles for six different tongue regions measured using high-speed video. As shown in the key and diagram below, six regions of the tongue exposed to nectar were labelled A–F, where A–C and D–F represent the ventral part and dorsal parts, respectively. The glossal hairs start to erect asynchronously, at 0 ms (regions A and D), 2 ms (region E), 3 ms (region B) and 28 ms (regions C and F). (B) Contact angles of different regions on the glossa surface in 25%, 35% and 45% (wt/wt) sucrose solution (n=9 bees). The glossa surface is more hydrophilic to the high concentration nectar, which is elucidated from the decreasing contact angles with increased nectar concentration (see supplementary material Table S2). The tongue tip is more hydrophilic, with smaller contact angles; the glossa have a descending order of hydrophilicity: C>B>A; the dorsal surface is also much easier to be wetted: D>A, E>B and F>C.

which ρ_{nec} is the density of the sucrose solution, $h(x)$ is the hair length, $\alpha(x)$ is the erection angle satisfying $0°\leq\alpha(x)\leq90°$, and X is the length of the tongue tip soaked in the nectar. The glossal hairs transform from their resting to erect postures during lapping, increasing the erection angles directly, thereby promoting the ability of nectar intake. From the formula of nectar intake mass listed above, we can speculate that if all of the hairs erect vertically, namely $\alpha(x)=90°$, the proboscis will ideally lift the largest amount of nectar, which can be calculated as $Q_{\max}=\rho_{nec}\int_0^X h^2(x)dx$. However, the average erection angle was 37.26°, which was not in accordance with the optimal erection angles. In our case, the viscous drag can be written as $F_v \propto \mu\cdot(2\pi\{r_0+h(x)sin[\alpha(x)]\})\cdot s(t)\cdot\dot{s}(t)$, where μ is the nectar viscosity, $s(t)$ is the displacement of the tongue, and r_0 is the radius of the glossal pad (Kim et al., 2011). The viscous drag equation suggests that if the erection angles are bigger, the drag together with the energy needed for overcoming drag will be larger. So honeybees may achieve an efficient energy-saving mechanism by adjusting the erection angles to balance the volume of trapped nectar and the energy used for overcoming viscous drag. The basal parts were immersed in nectar for the shortest time compared with the anterior and middle parts, so hairs of section I need to perform rapid erection to take more nectar. Intriguingly, both the erection angles and hair length on the proximal segment were greater than those on sections II and III, which increased the amount of lifted nectar and overcame the shortcomings of the lower wettability of basal hairs. In addition, the anterior tongue was the most hydrophilic, so prolonging the time immersed in the nectar might improve the amount of trapping sugar water. It is likely that the dynamic surface of the honeybee's glossa helps *Apis mellifera ligustica* make use of a limited nectar resource to accommodate the energy-intensive lifestyle (Harper et al., 2013). The honeybee's asynchronous erection and section-wise wettability properties of glossal hairs for nectar feeding could serve as valuable models for developing miniature viscous micropumps that are both protrusible and have a highly dynamic hydrophilic surface (Amirouche et al., 2009).

MATERIALS AND METHODS

Specimen collection and processing

The honeybee (*Apis mellifera ligustica* Spinola 1806) specimens were collected from Beijing, China (40.00°N, 116.33°E) and housed in a beehive, where the temperature and humidity were maintained at 25°C and 50%, respectively. Supplementary material Fig. S1 shows one honeybee specimen used in our experiments. We confirmed that no specific permissions were required for these locations and activities, and the field studies did not involve endangered or protected species. Three types of experiment, namely observation of surface microstructure on the glossa, acquisition of hair erection kinematics and wettability in different sections of glossa, were performed. To remove chemical contamination of the mouthparts, unfed, laboratory-reared specimens were handled with latex gloves. Ten glossa specimens of worker bees were selected, fixed in a 2.5% glutaraldehyde solution, dehydrated in an ethanol series (75%, 80%, 85%, 90%, 95%, 100%, approximately 30 min each), and coated in gold palladium and observed under a scanning electron microscope (SEM, FEI Quanta 200, Czech Republic); average length of these tongues was 2.5 mm. Supplementary material Fig. S2 shows detailed information about the mouthpart structure and morphology and the sizes of the glossal hairs directly measured in SEM figures.

Observation of the honeybee drinking process

The experimental setup for observing the drinking process comprised a positioner, a glass feeder filled with artificial nectar (sucrose solution), a white 100 W light source and a high-speed camera (Olympus, iSpeed TR, Japan, up to 2000 frames per second) with a microscope (Keyence, VH-Z50L, Japan, up to the magnification of ×50) (Fig. 1A; supplementary material Fig. S3). The positioner, actuated by a servo-motor, could move up and down with the motion accuracy of 1 µm. The honeybees were starved for 24 h before the drinking process observation experiment. Then, the live honeybee was glued to the precision positioner via its thorax so it could be moved vertically, thereby allowing its mouthpart to reach the level of the artificial nectar. We filmed a honeybee drinking a 35% (wt/wt) sucrose solution from a lateral shooting angle at a frequency of 500 frames per second (Kim et al., 2011) (see supplementary material Movie 1). The images in different regions of glossa were captured by adjusting the height of the positioner. A series of high-resolution photographs captured by the high-speed camera in every microsecond were processed via Matlab (R2013b, MathWorks, Natick, MA, USA). In order to ensure the repeatability and correctness of the hair erection results during nectar feeding, we captured nine videos in total, in which we selected three worker bee samples and each of them contributes to three entire drinking cycles. For one strand of glossal hair, the Canny Operator was used to extract its profiles, and two vectors, τ_1 and τ_2, could be obtained to represent the direction between the glossal hair and the tongue's long axis, respectively. We then calculated the erection angles using the formula $\alpha(x)$=across $[(\tau_1\cdot\tau_2)/(\|\tau_1\|\cdot\|\tau_2\|)]$. Erection angles of 10 hairs in one region were selected randomly as $\alpha_i(x)$ (i=1, 2…10), to

calculate the average erection angles on different regions of glossa, depicted as: $\alpha_I(x) = \sum_{i=1}^{10} \alpha_i(x)/10 (I = A,B,C,D,E,F)$.

Wettability measurements

To measure the wettability of the tongue tip, a glossa specimen was first vertically attached on a paraffin cubic, then it pierced a nectar–air interface and a meniscus formed around it (Lehnert et al., 2013). The video recorded the shape of the meniscus while lowering the nectar level at a very low speed of 0.0125 mm s^{-1} at which the quasi-static situation was simulated. Shown in Fig. 1B,E, the meniscus met the glossa surface at a contact angle $\theta(x)$, which was determined by the microstructure of the surface and the material chemistry of the glossa (Fig. 1E). The meniscus approached a horizontal nectar–air interface as the distance from the glossa increased; the shape of the meniscus and its height were the important factors that allowed the glossa wettability to be evaluated. The contour of the meniscus was recorded using the high-speed camera while the nectar was continuously lowered by the positioner. The contact angles were calculated by processing a series of high-speed images via Matlab (R2013b, MathWorks), in different sections to ensure the repeatability of the data. Contact angles in different parts of regions I–III are shown in supplementary material Table S2.

Calculation of erection angles

The high-speed photography gave us a series of images representing the glossal hair behavior per microsecond. We measured the erection angles of the glossa directly from the images. For one strand of glossal hair, as shown in supplementary material Fig. S4, the two vectors τ_1 and τ_2 can be obtained by connecting two pairs of key points, namely, P and Q, R and S, which represent the direction between the glossal hair and the tongue's long axis, respectively. We then calculated the erection angles using the formula $\alpha(x) = \arccos\frac{\tau_1 \cdot \tau_2}{\|\tau_1\| \cdot \|\tau_2\|}$. Three independent drinking cycles are measured and the data of erection angles in parts A–F are shown in supplementary material Table S1.

Acknowledgements

We thank the Centre of Biomedical Analysis of Tsinghua University for their assistance with the specimen processing and SEM image capturing.

Competing interests

The authors declare no competing or financial interests.

Author contributions

All authors discussed and commented on the manuscript. S.Y., J.W. and Y.Y. conceived the project. S.Y. and J.W. planned and performed the experiments. J.W. and R.Z. analyzed the data, and J.W., S.Y. and R.Z. wrote the paper.

Funding

This study was funded by the National Natural Science Foundation of China (Grant no. 51475258) and a Research Project of the State Key Laboratory of Tribology (Grant no. SKLT11B03).

Supplementary material

Supplementary material available online at
http://jeb.biologists.org/lookup/suppl/doi:10.1242/jeb.111013/-/DC1

References

Amirouche, F., Zhou, Y. and Johnson, T. (2009). Current micropump technologies and their biomedical applications. *Microsyst. Technol.* **15**, 647-666.
Crompton, A. W. and Musinsky, C. (2011). How dogs lap: ingestion and intraoral transport in *Canis familiaris*. *Biol. Lett.* **7**, 882-884.
Harper, C. J., Swartz, S. M. and Brainerd, E. L. (2013). Specialized bat tongue is a hemodynamic nectar mop. *Proc. Natl. Acad. Sci. USA* **110**, 8852-8857.
Heyneman, A. J. (1983). Optimal sugar concentrations of floral nectars? dependence on sugar intake efficiency and foraging costs. *Oecologia* **60**, 198-213.
Kim, W., Gilet, T. and Bush, J. W. M. (2011). Optimal concentrations in nectar feeding. *Proc. Natl. Acad. Sci. USA* **108**, 16618-16621.
Kim, W., Peaudecerf, F., Baldwin, M. W. and Bush, J. W. M. (2012). The hummingbird's tongue: a self-assembling capillary syphon. *Proc. R. Soc. B.* **279**, 4990-4996.
Krenn, H. W., Plant, J. D. and Szucsich, N. U. (2005). Mouthparts of flower-visiting insects. *Arthropod. Struct. Dev.* **34**, 1-40.
Lehnert, M. S., Monaenkova, D., Andrukh, T., Beard, C. E., Adler, P. H. and Kornev, K. G. (2013). Hydrophobic-hydrophilic dichotomy of the butterfly proboscis. *J. R. Soc. Interface* **10**, 20130336.
Reis, P. M., Jung, S., Aristoff, J. M. and Stocker, R. (2010). How cats lap: water uptake by *Felis Catus*. *Science* **330**, 1231-1234.
Rico-Guevara, A. and Rubega, M. A. (2011). The hummingbird tongue is a fluid trap, not a capillary tube. *Proc. Natl. Acad. Sci. USA* **108**, 9356-9360.
Snodgrass, R. E. (1956). *Anatomy of the Honey Bee*, pp. 59-93. New York: Comestock Publishing Association, Ithaca.
Song, C. and Zheng, Y. (2014). Wetting-controlled strategies: from theories to bio-inspiration. *J. Colloid Interf. Sci.* **427**, 2-14.
Tan, K., Latty, T., Hu, Z., Wang, Z., Yang, S., Chen, W. and Oldroyd, B. P. (2014). Preferences and tradeoffs in nectar temperature and nectar concentration in the Asian hive bee Apis cerana. *Behav. Ecol. Sociobiol.* **68**, 13-20.
Yang, H., Wu, J. and Yan, S. (2014). Effects of erectable glossal hairs on a honeybee's nectar-drinking strategy. *Appl. Phys. Lett.* **104**, 263701.4.

Fig. S1. Honeybee specimen of *Apis mellifera ligustica*.

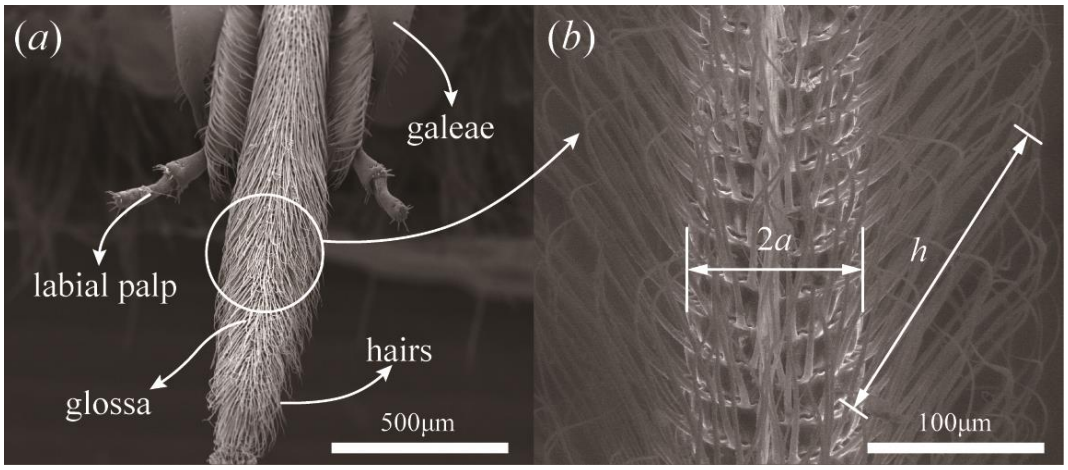

Fig. S2. The honeybee's mouthpart. (a) The mouthpart consists of a pair of labial palpi, a pair of galeae and a glossa covered by dense hairs. (b) The enlarged part of a typical glossa with bushy hairs. We measured and averaged lengths of the glossal hairs in Regions I~III. The lengths of the glossal hairs are 109.47 ± 8.96 μm, 110.57 ± 5.97 μm, 126.61 ± 13.73 μm, respectively.

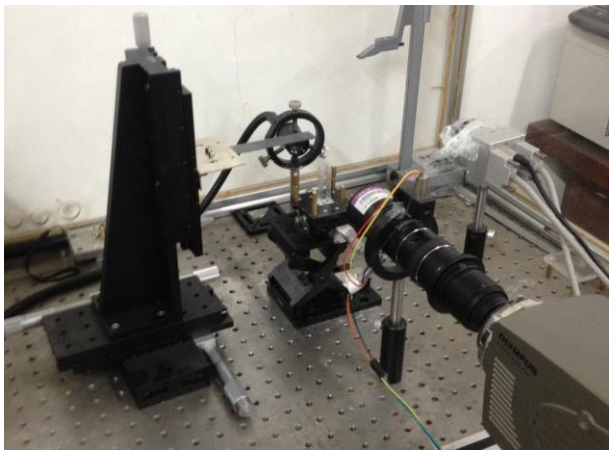

Fig. S3. The experimental setup

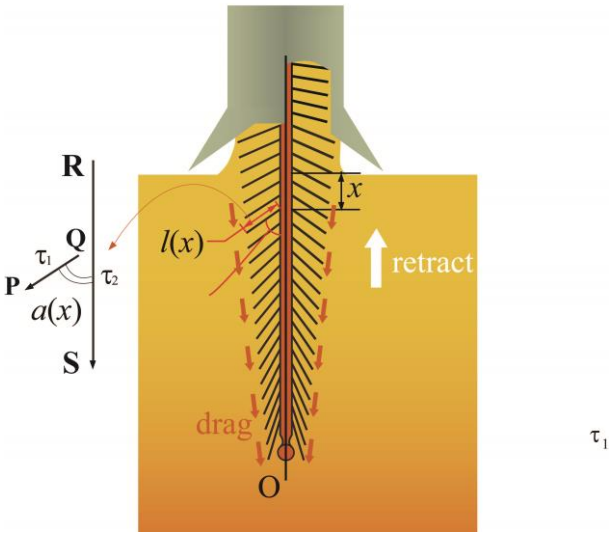

Fig. S4. Calculation method of the erection angle.

Movie 1. Dipping behaviour of a honeybee.

Table S1. Data of erection angles measured from high-speed images and then converted to real sizes

t / ms	Part A		Part B		Part C		Part D		Part E		Part F	
	Ave.	St. Dev	Ave.	St. Dev	Ave.	St. Dev	Ave.	St. Dev	Ave.	St. Dev	Ave.	St. Dev
0	5.00	0.00	0.00	0.00	0.00	0.00	5.00	0.41	0.00	0.00	0.00	0.00
1	10.08	1.81	0.00	0.00	0.00	0.00	10.30	0.93	0.00	0.00	0.00	0.00
2	11.00	1.23	0.00	0.00	0.00	0.00	11.36	0.14	3.78	0.06	0.00	0.00
3	18.48	0.22	3.00	0.00	0.00	0.00	18.11	1.65	13.24	0.16	0.00	0.00
4	24.62	0.99	5.00	0.00	0.00	0.00	28.21	1.78	18.25	0.91	0.00	0.00
5	26.22	1.54	9.00	0.00	0.00	0.00	28.19	0.28	15.52	1.49	0.00	0.00
6	28.44	1.23	14.04	0.00	0.00	0.00	31.41	0.87	16.00	0.54	0.00	0.00
7	29.48	0.97	14.62	0.00	0.00	0.00	32.79	1.79	16.76	0.98	0.00	0.00
8	30.98	0.61	16.50	0.00	0.00	0.00	32.11	3.07	16.60	0.37	0.00	0.00
9	30.45	0.30	18.43	0.00	0.00	0.00	31.47	3.04	19.15	1.44	0.00	0.00
10	30.45	0.83	19.18	0.00	0.00	0.00	32.91	0.52	19.77	0.50	0.00	0.00
11	30.65	1.76	19.65	0.00	0.00	0.00	30.96	3.01	21.37	1.08	0.00	0.00
12	31.61	1.68	20.32	0.00	0.00	0.00	32.28	3.09	22.25	1.56	0.00	0.00
13	30.65	1.00	21.04	0.00	0.00	0.00	31.57	1.53	21.04	1.87	0.00	0.00
14	31.61	1.67	21.04	0.00	0.00	0.00	32.68	2.62	21.38	2.05	0.00	0.00
15	31.83	0.90	20.77	0.00	0.00	0.00	32.01	0.45	20.22	1.11	0.00	0.00
16	32.20	0.48	21.45	0.00	0.00	0.00	31.33	1.32	22.83	0.32	0.00	0.00
17	31.61	1.76	21.20	0.27	0.00	0.00	32.55	2.98	22.25	0.33	0.00	0.00
18	32.62	1.89	23.11	0.41	0.00	0.00	32.97	2.61	23.75	0.61	0.00	0.00
19	30.96	1.17	23.43	0.26	0.00	0.00	32.47	3.12	23.50	1.98	0.00	0.00
20	31.83	0.18	24.15	0.53	0.00	0.00	31.76	2.08	23.97	0.61	0.00	0.00
21	31.83	1.42	22.93	1.89	0.00	0.00	33.02	0.12	23.76	1.93	0.00	0.00
22	30.38	3.38	21.80	1.05	0.00	0.00	32.70	2.78	24.62	0.60	0.00	0.00
23	31.26	3.34	22.48	0.95	0.00	0.00	32.26	3.01	25.56	2.38	0.00	0.00
24	31.61	4.03	22.75	0.81	0.00	0.00	33.07	2.24	25.46	0.89	0.00	0.00
25	32.18	3.97	22.75	0.52	0.00	0.00	34.45	2.61	25.99	0.51	0.00	0.00

Table S2. Contact angles at different regions of the bee tongue

concentration	A		B		C		D		E		F	
	Ave.	St. Dev	Ave.	St. Dev	Ave.	St. Dev	Ave.	St. Dev	Ave.	St. Dev	Ave.	St. Dev
25%	55.55	0.70	48.20	1.20	41.95	0.90	51.94	0.70	49.23	0.40	36.91	0.70
35%	43.49	0.50	38.50	0.30	35.20	0.30	41.25	0.50	35.77	0.80	32.30	0.60
45%	42.02	0.50	36.82	0.80	29.21	0.50	35.74	0.30	31.6	0.40	24.70	1.00